Arizona Geological Society Digest 22
2008

Cenozoic tectonic history of the northern Sierra Madre Occidental, Huizopa, Sonora-Chihuahua, Mexico

Joseph Andrew
Alaska Division of Geological and Geophysical Surveys, 3354 College Rd., Fairbanks, Alaska, 99709

ABSTRACT

The Sierra Madre Occidental of northwestern Mexico is usually noted for vast volumes of rhyolitic tephra and related calderas emplaced in the Oligocene and little internal deformation. Recent fieldwork from an isolated area, along the Rio Huizopa, within the regionally mapped Sierra Madre Occidental found no calderas or ignimbrites but identified many faults. An approximately one to two kilometer thick section of basaltic lava flows occurs with a few intervening volcaniclastic units. The bottom and top of this volcanic pile are not exposed in the study area and the true thickness may be much greater. The strata can be divided into three major lava flow successions separated by volcaniclastic units; the lower and middle successions are basalt, the middle is bimodal with basalt and local rhyolite lavas, and the uppermost succession basaltic-andesite and andesite lavas. A thick rhyolitic lava unit occurs locally, with a probable thickness over one kilometer. No geochronology data exist for this area; these volcanics are probably similar in age to the Oligocene volcanics in the rest of the Sierra Madre Occidental. Mafic to intermediate dikes commonly cut all of the strata with dominantly north-northwest trends. At least one locality exposes feeder dikes into a volcano edifice forming a triple junction dominated by north-northwest dikes. This entire volcanic package is tilted so that most units dip moderately to the west.

Numerous faults cut all of these volcanics. The most conspicuous fault set is a system of silicified normal faults with dominantly moderate eastward dips, although a north set dips westward. These faults have well-developed breccia and slickensides and steep rakes of slickenlines. Steeply dipping hanging wall faults are common. The breccia systems along these faults have spectacular multiple brecciation textures recording repeated episodes of fault movement breccia creation and breccia silicification. These major faults have an overall corrugated shape on scales of tens of centimeters to hundreds of meters, but detail is limited due to generally poor exposures and dense vegetation. These faults cut all of the volcanic units exposed here. The mean trend of the fault striae is east-northeast, but other several distinct fault striae sets occur on these fault planes; a set of northerly trends and east-west trends. Based on cross-cutting relationships of multiple overprinting fault striae both of these other striae sets are due to a later deformation events reactivating the normal faults. The northerly-trending striae have low rakes with right-lateral shear. The next most conspicuous fault set occurs here as subvertical north-northwest trending strike-slip faults with right-lateral displacement. Several of these faults have tens of centimeters thick gouge zones specifically where they cut the north-trending faults.

These fault and dike structures record a change in tectonic strain from north-north-east extension during and just after Oligocene volcanism to east-west extension then to northerly

e-mail: joseph.andrew@alaska.gov

Andrew, Joseph, 2008, Cenozoic tectonic history of the northern Sierra Madre Occidental, Huizopa, Sonora-Chihuahua, Mexico, *in* Spencer, J.E., and Titley, S.R., eds., Ores and orogenesis: Circum-Pacific tectonics, geologic evolution, and ore deposits: Arizona Geological Society Digest 22, p. 517-528.

trending right-lateral shear. This tectonic history is roughly similar to the regional tectonic history derived from studies in Sonora, Chihuahua and Arizona. The strong episode of metamorphic core complex formation in Arizona and Sonora may be related temporally and tectonically to the prominent normal faults in the Rio Huizopa region.

INTRODUCTION

The Cenozoic tectonic evolution of the Sierra Madre Occidental (Fig. 1) has been portrayed in available geologic literature as dominated by rhyolitic calderas and ignimbrites and little deformation, despite being surrounded by provinces that have experienced strong Cenozoic deformation (McDowell and Keizer, 1977; Stewart, 1978, 1998; Henry and Aranda-Gómez, 1992, 2000). Most previous workers have hypothesized that this geologic province has unique properties that have inhibited deformation. However, the study of the area has been hampered by difficult access in rugged areas with few roads. Has this difficulty of access inhibited geological study and caused researchers to apply the limited observations from areas near roads to characterize the province as a whole?

This paper presents new geologic data collected from a key locality, the Rio Huizopa, in the northern Sierra Madre Occidental. This new data are used to characterize and evaluate the regional tectonic evolution of this area. The northern Sierra Madre Occidental and nearby areas are currently of interest to gold and precious metal exploration. New gold mines have recently began mining, located to the northeast and southwest of Rio Huizopa, Dolores and Mulatos, respectively. These two mine areas and Huizopa itself have been mined and prospected historically, but no published study has examined the tectonic evolution of this area. The tectonic evolution is ultimately responsible for creation of structures that provided pathways for mineralizing fluids emanating from the thermal and hydraulic sources of mineralization.

The nearest road to Rio Huizopa is a five-hour horseback ride away. No previous geologic data exists for this area except 1:250,000 regional mapping (Servicio Geológico Mexicano, 2000). These regional maps show voluminous deposits of relatively mafic lavas with lesser volumes of rhyolite lava or local ignimbrite. The area is ideal for study because it is near the boundaries of the Sierra Madre Occidental, Gulf Extensional, and Southern Basin and Range provinces and could preserve multiple deformation events. Strong stream incision in this region creates good exposures with large topographic and thus structural/stratigraphic relief. Servicio Geológico Mexicano (2000) mapped several faults which may strike through the study area. The current study examines the

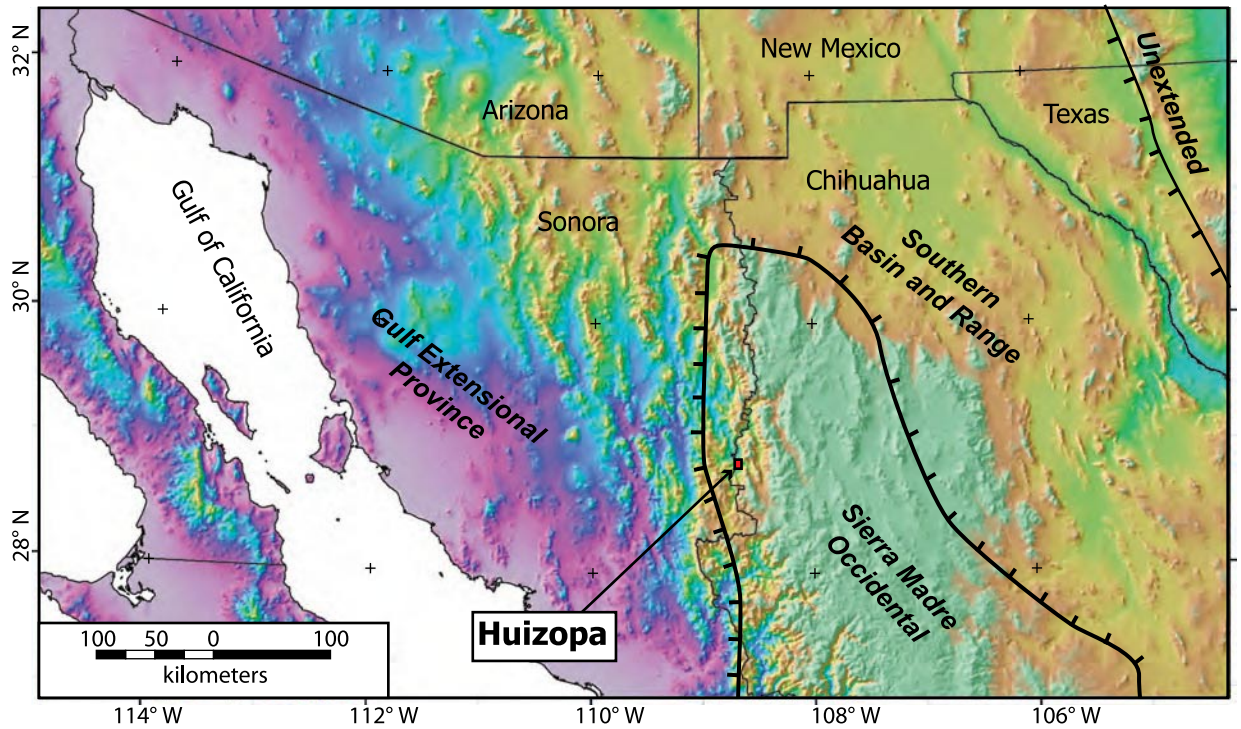

Figure 1. Digital elevation map showing the location of the Rio Huizopa study area in the northern Sierra Madre Occidental and geologic province boundaries (provinces and boundaries from Dickinson, 2006). The limits of strong Cenozoic extension are denoted by the hachured thick lines.

faulting and associated deformation to investigate hypotheses of multiple, overprinting deformation events during Cenozoic time that are known to have affected the surrounding regions [see summaries in Gans (1997), Henry and Aranda-Gómez (2000), Ferrari et al. (2007)].

METHODS

New detailed (1:10,000 to 1:5000 scale) mapping and structural data were collected from a remote site along the Rio Huizopa in the northern Sierra Madre Occidental (Fig. 1). Access to this area is difficult and generally limited to horseback, helicopter, or small airplanes landing on a primitive landing strip. The topographic base map used for field work, with 2.5-meter topographic-contour intervals, was derived from aerial photographs flown by the gold exploration company Minera Sol de Oro S.A. All of the map data were input into a geographic information systems (GIS) database for creation of the final map. Structural analyses and stereographic plots were made using Stereonet and FaultKinWin software by R. Allmendinger.

OBSERVATIONS

Rock units

The rocks in the Rio Huizopa study area are entirely volcanic or volcaniclastic (Fig. 2) with a local veneer of alluvium or colluvium. The volcanic sequence is probably Oligocene in age, as is much of the surrounding region (Servicio Geológico Mexicano, 2000), but no rocks within this study area have been dated.

The volcanic/sedimentary sequence is essentially bimodal with basalt and basaltic-andesite lava flows dominating the lower and upper sections with a middle sequence of rhyolite. Rhyolite is spatially limited to two relatively thick exposures in the map area: the northern one has a thickness of possibly >400 m, and another rhyolite in Arroyo Placitas a smaller and thinner. The rhyolite typically has strong flow foliation with numerous folds of foliation, including recumbent isoclinal and sheath folds. The foliation of the rhyolite generally parallels the lower contacts, but locally, especially in Arroyo Placitas, the foliation is subvertical. Local coarse pumice breccia and obsidian layers occur near the base and top. The lower contact of the rhyolite grades downward into tuffaceous deposits. All of these observations lead to an interpretation of rhyolite lava flows (using the criteria of Fink and Manley, 1987). Exposures beyond the lava dome complexes the two the lava flows are generally 5-10 m thick. Two stratigraphically separate rhyolite lava flows are exposed between the lava domes, with an intervening succession of basaltic lava flows and volcaniclastics (Fig. 3). These two rhyolite flows are similar enough that they cannot be distinguished from each other except by stratigraphic position. The flows are probably from the two domes but the flows cannot be attributed to either dome due to discontinuous exposures. The intervening basaltic and volcaniclastic deposits seem to pinch out into the northern rhyolite dome. The upper basaltic-andesite lava flow sequence, above the rhyolites, is similar to the lower volcanic sequence, but the upper portion of the sequence has lava flows of more andesitic compositions. The andesite flows are thicker and lighter in color and cap many of the ridge tops.

Volcaniclastics are interbedded with the lava-flow sequences and some of these are large enough to be mapped separately (Fig. 2). The clasts of the volcaniclastic sediments are similar in composition to the interbedded lava flows. A conspicuous white-colored volcaniclastic unit outcrops along the Rio Huizopa in an otherwise basaltic and basaltic volcaniclastic dominated section. This white volcaniclastic unit is composed of rhyolitic clasts in a tuffaceous matrix, which may be derived from the thick rhyolitic lava flow sequence present to the north and west. Locally, foliated rhyolite occurs directly on top of this white volcaniclastic unit.

Primary structures

The average bedding and flow foliation for these volcanic and volcaniclastic units, exclusive of the rhyolite foliations, dip to the west-southwest at approximately 25° (Figs. 4a). The rhyolite flows have contorted and folded foliations that range from subhorizontal to subvertical and they account for much of the scatter in Figure 4a. Numerous dikes intrude all of these units (Fig. 2), ranging in composition from mafic to felsic with dominant north-northwest strikes and steep dips (Fig. 4b). One locality at the north end of the map area (Fig. 2) has a triple-junction geometry of radiating dikes that appear to be a volcanic feeder zone for one of the upper mafic flows.

Secondary structures

Joints are common features cutting across all of the volcanic and volcaniclastic units mapped. The joints are most abundant in the immediate hanging walls of several large normal-fault systems (see the next section on faults). Joints generally strike north-northwest and dip steeply eastward (Fig. 4c), although there is considerable scatter and several subgroups of orientations. Veins of calcite and quartz are also common near the large normal fault structures and have an overall similar trend (Fig. 4d) to the dikes and joints (Figs. 4b and c), but there is also scatter to several other orientations.

Many fault sets (Figs. 4e, f, g, and h) occur in the Rio Huizopa area, most notable of which are north-northwest striking, moderately east-northeast dipping (mean dip = 42°, Fig. 4e) normal faults. Four of these normal fault systems occur in the study area (Fig. 2): two in Arroyo Adelina (Fig. 5), and one each in Arroyo Agua Escondida and Arroyo Las Placitas. The structures in Arroyo Adelina continue into an historic gold mining site in the canyon bottom of Rio Huizopa. Silicified breccias occur along these normal faults, which record multiple cycles of brecciation and silicification.

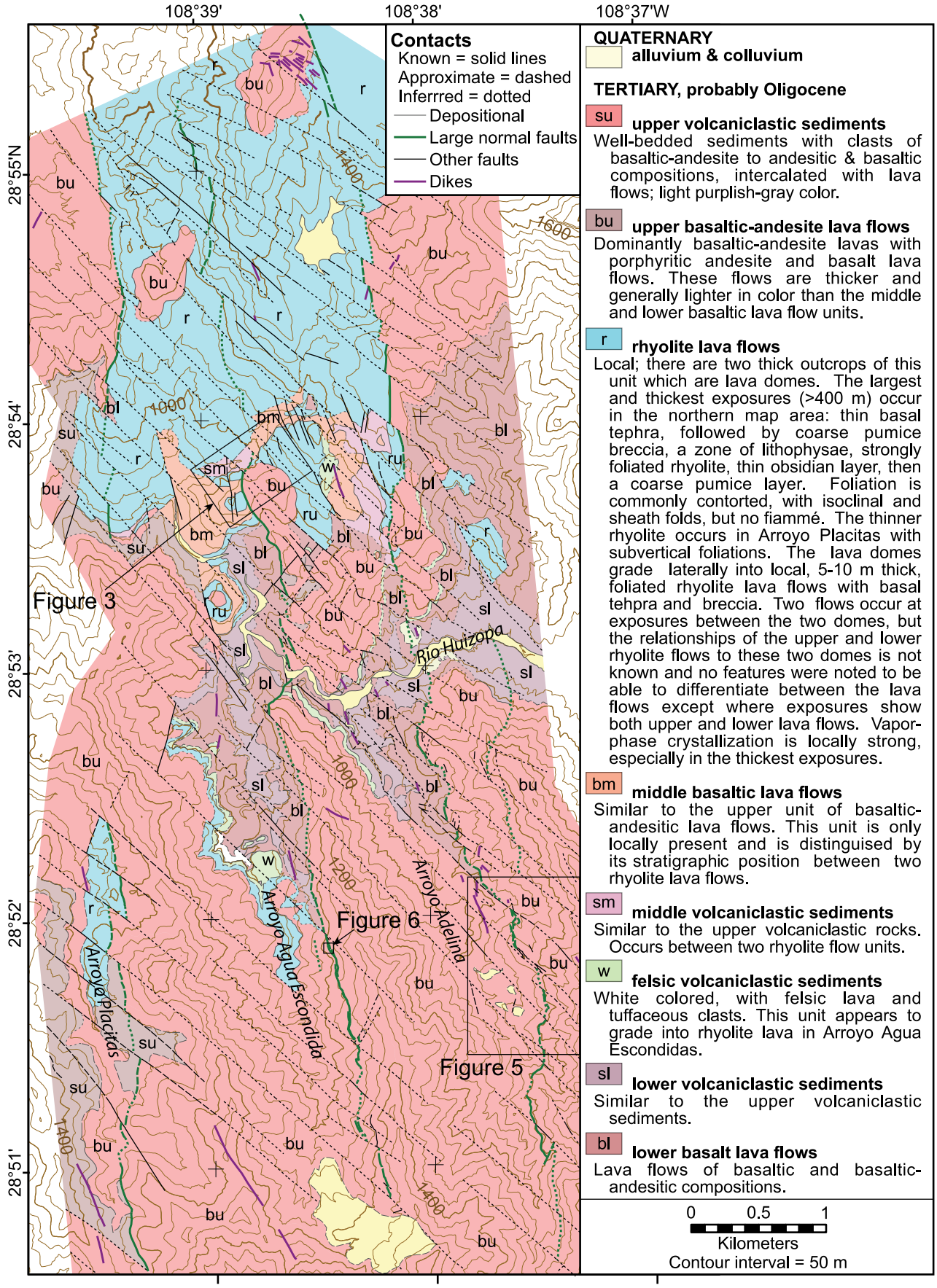

Figure 2. Simplified geologic map of the Rio Huizopa area, showing the stratigraphic units and major faults. Note the apparent left-lateral offset of the northerly-striking, large normal faults by northwest-striking, steep-dipping faults.

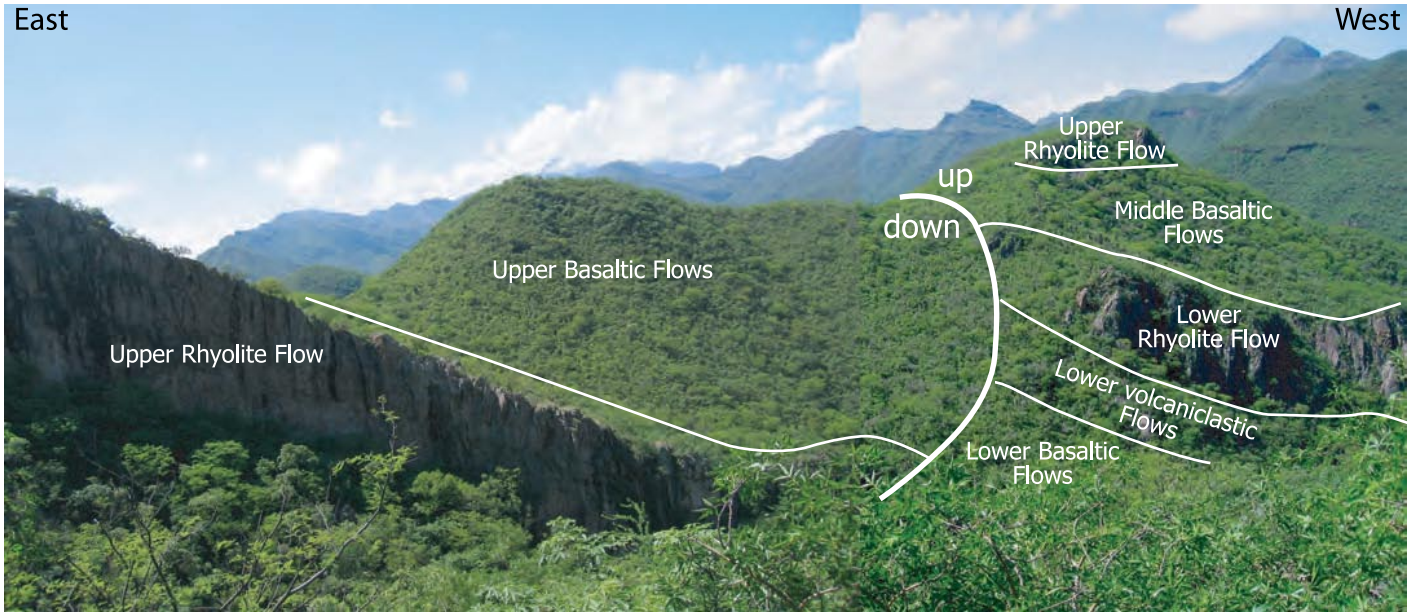

Figure 3. Southward-looking view of offset along a large normal fault in Rio Huizopa (northward continuation of the normal fault in Arroyo Agua Escondida). The upper rhyolite flow is offset by ~190 meters, down to the east. Note the topographic relief in the background and the dense, monsoon-related vegetation. This vegetation limits the amount and quality of geologic exposures.

These normal fault systems have displacements of hundreds of meters based on offset stratigraphic units (Fig. 3). Such a significant amount of displacement is supported by observations of tens of centimeters of gouge along some of these structures. A set of steeply dipping, synthetic and antithetic faults occur in the hanging wall and sometimes in the footwall of the large normal faults.

The large normal fault zones are conspicuous features forming resistant ridges (Fig. 6) due to the intense silicification along them and the clay alteration of the surrounding rocks. These fault zones in the areas of dominantly basaltic-andesite seem to hold up the ridges: each of the three main north-south valleys have one or more of these east-dipping faults on their eastern flanks. These fault zones can easily be followed along strike on west-facing slopes, but they are often offset to the left and downhill (Fig. 5). These offsets occur on northwest-striking, steep to moderately dipping, non-silicified faults. These faults are not well-represented in the field data collected (Fig. 4i) because they are not silicified and tend to be altered so they are low areas that are covered by alluvium and colluvium. The apparent offsets of the large normal fault zones could result from north-side down dip-slip movement or left-lateral strike-slip movement, which matches with the normal fault displacements (Fig. 4i) found at the few measured exposures of these cross-cutting faults.

One other prominent set of faults also cuts the large normal fault zones (Figs. 2 and 4f). These are steeply dipping, northerly striking faults with right-lateral sense of shear. These features are parallel to the strike of the large normal faults and their associated synthetic and antithetic faults. There are several other less-common sets of faults (Fig. 4f and h) of normal, oblique and strike-slip kinematics.

The exact relative timing of the different fault sets is difficult to ascertain due to the generally poor exposures of non-silicified faults. The large, silicified normal faults are definitively cut by younger faults, both the northerly striking right-lateral faults and the northwest-striking normal faults. The timing relationships between these younger faults is less certain. The offsets of the northwest-striking normal faults are more conspicuous and thus can be more easily mapped (Figs. 2 and 5). The northerly-trending right-lateral strike-slip faults have similar strikes to the silicified normal faults so that they are overshadowed by the strain related to the large normal faults and so are less easily mapped. Many of these strike-slip faults seem to be reactivated antithetic and synthetic faults to the earlier normal faults.

ANALYSIS

Faults and striae

Distinct deformation patterns are not very clear from plots of fault striae (Fig. 4h). Numerous orientations of fault striae can result from one stress vector applied to many faults with diverse orientations. A simplistic Mohr-Coulomb stress-strain fault model can have normal, thrust, right-lateral strike-slip and left-lateral strike-slip faults at different orientations. Complicated patterns of fault striae may also be caused by multiple deformation events that overprint or reactivate earlier formed faults.

The fault striae data can be analyzed using by creating subgroups using the fault striae rakes, dividing the faults into: strike-slip, oblique and dip-slip faults. Strike-slip striae (rakes < 30°) occur on mostly northerly-striking, steeply to

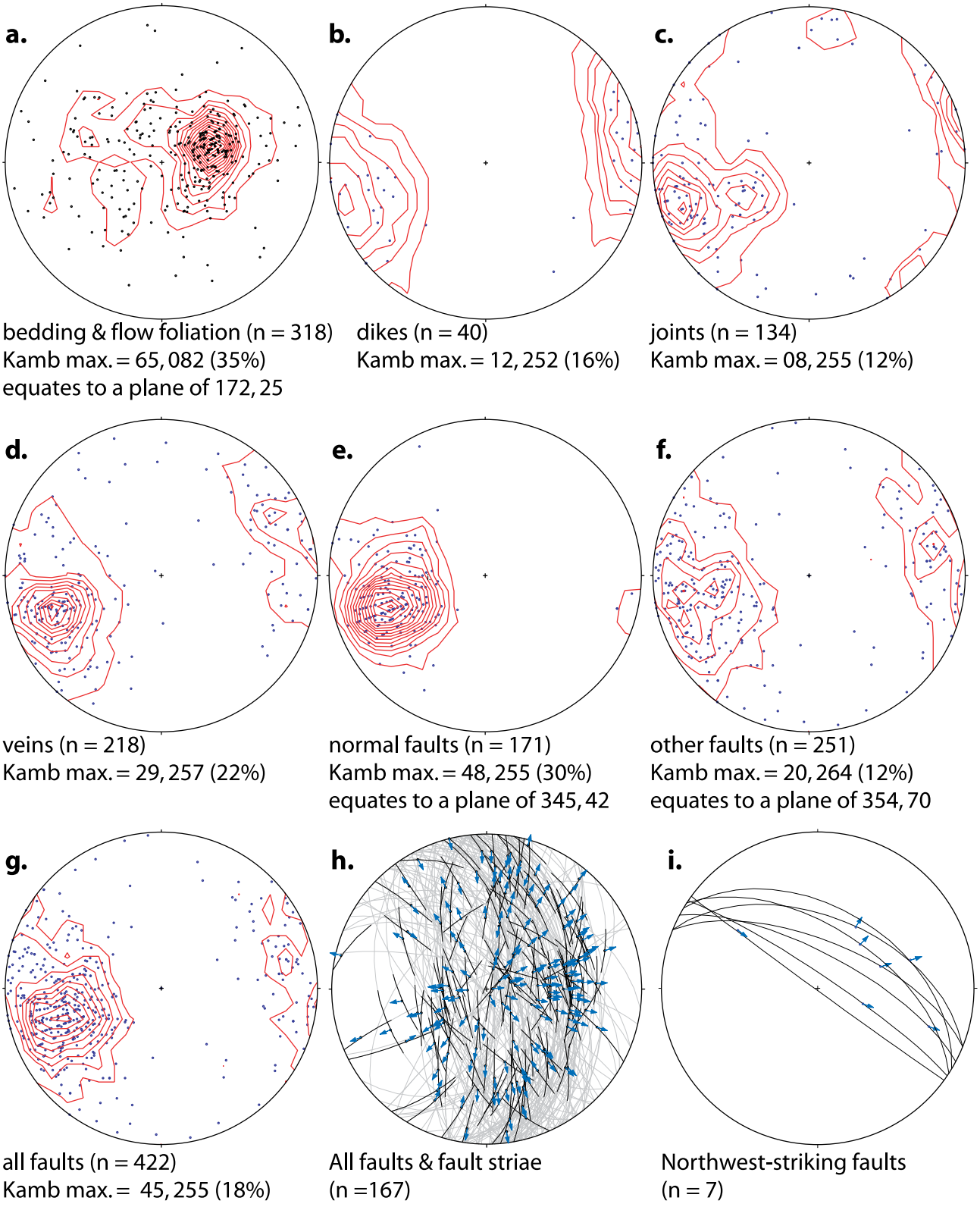

Figure 4. Lower hemisphere equal-area stereograms of primary and secondary structures. The red lines are Kamb contouring at a significance of 2 in 2% contours, created using StereoWin by R. Allmendinger. The 'Kamb max.' referred to on each plot is the plunge, trend and contour amount at the maximum Kamb contour of the data. 4a. Stereograph of poles to bedding & flow-foliation. 4b. Poles to dikes. 4c. Poles to joints. 4d. Poles to veins. 4e. Poles to large normal faults. 4f. Poles to other faults. 4g. Poles to all faults. 4h. Great circle faults with measured fault striae. The fault striae are shown by blue arrows which point in the direction of hanging wall transport relative to the footwall. The fault planes for each fault striation are shown by the light gray great circles with the segment around the striae orientation highlighted in black. 4i. Great circles of northwest and southeast striking subset of faults with measured fault striae.

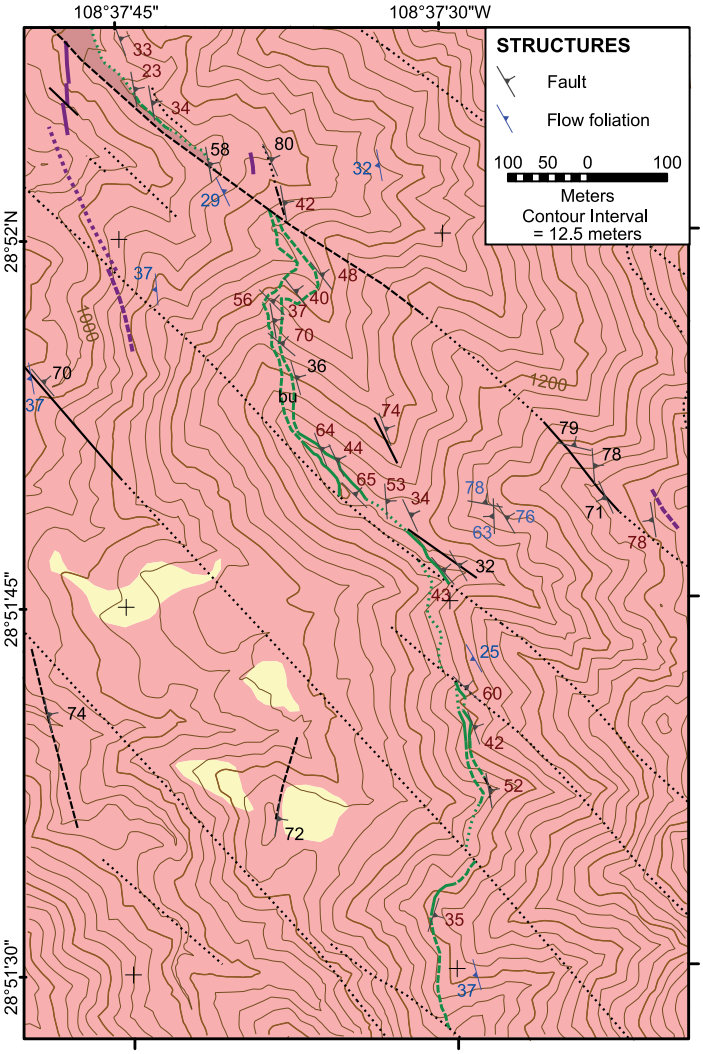

Figure 5. Detailed geologic map of Arroyo Adelina showing shallowly east-dipping normal fault system off by numerous, steeply-dipping north-northwest-striking faults (see Figure 2 for location and symbol key). Note that data for fault striae, joints and veins are not shown.

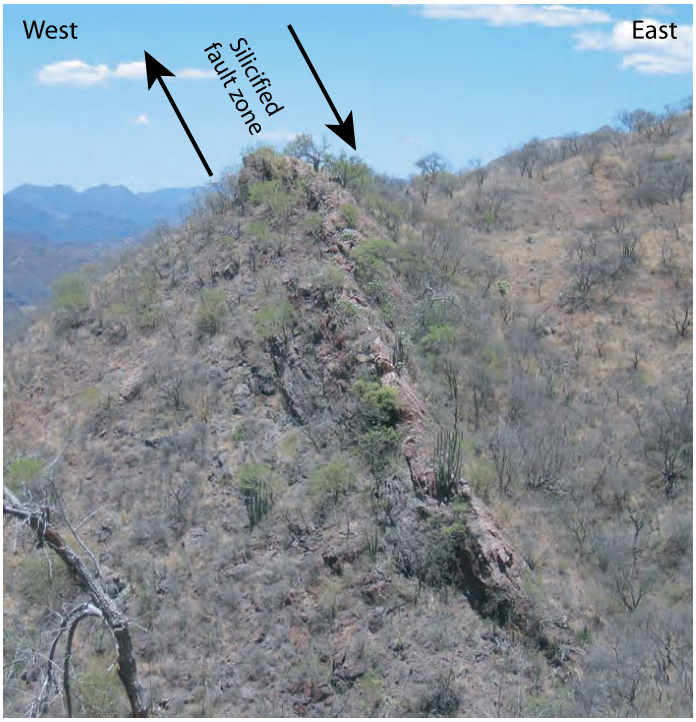

Figure 6. Northward-looking view of a large, silicified normal fault zone exposed along the eastern side of Arroyo Agua Escondida. The upper surface of the fault zone is very planar and has abundant steeply-plunging fault striae and sub-parallel mullions. The view is approximately 50 meters across. Note the sparse non-monsoon vegetation.

moderately dipping faults (Fig. 7a). A lesser number of strike-slip striae occur on northwest or northeast striking, steeply dipping faults. Oblique fault striae are relatively abundant, representing a third of the measured striae (Fig. 7b). Oblique striae occur on many orientations of faults with the most prevalent orientations being northeast-striking, moderately southeast-dipping and steeply dipping, northerly striking faults. Dip-slip striae (rakes > 60°) occur on several sets of faults (Fig. 7c). The most numerous dip-slip striae occur on northerly-striking faults which dip moderately to gently eastward. Another set of dip-slip striae occur on southerly-striking, steeply west-dipping faults. The rest of the dip-slip faults are sub-vertical faults which strike northwest and northeast.

The sense of shear of the striae can also be used to make subsets of the kinematic data. These subsets were created by separating the kinematic data of the dominantly strike-slip fault striae (rake < 45°) into right- and left-lateral sense of shear. This analysis yields a distinct relationship of the orientation to the sense of shear: striae with right-lateral sense of shear occur on steeply to moderately east-dipping, north-striking faults and on northwest-striking, variable-dip faults (Fig. 7d); while striae with left-lateral kinematics on northeast-striking, variable dip faults (Fig. 7e).

Paleostress axes

A more meaningful analysis can be done using paleostress orientations. The orientation of the three principal stress vectors needed to create the observed fault slip were calculated from fault plane and striae data using FaultKinWin of R. Allmendinger. There are distinct patterns of the minimum and maximum compressive stress vectors, the T and P axes, respectively (Fig. 7f). Most P-axes are steeply plunging, with dispersions to shallowly-plunging north-northeast and south-southwest trends. The T-axes show multiple concentrations in Figure 7f, the greatest of which is at shallow plunges trending east-northeast to west-southwest. The P and T-axes of the rake and kinematic subsets helps distinguish these maxima of stress axes (Fig. 7a-e). The dip slip striae have a strong concentration of T-axes trending east-northeast with a very shallow plunge (Fig. 7c). Oblique striae show two maxima: shallowly

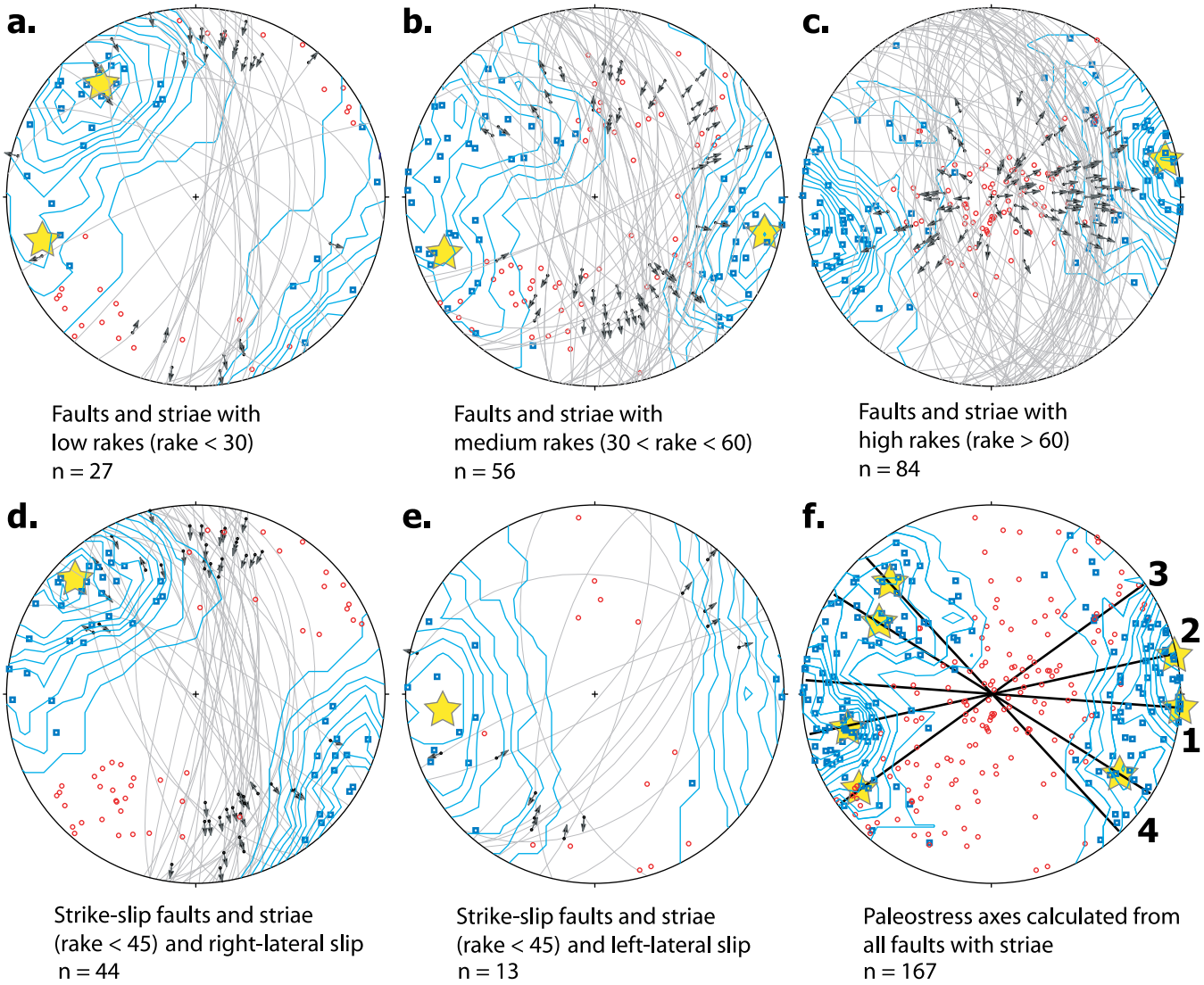

Figure 7. Stereograms of kinematic subsets of fault and striae couplets. Faults are shown as great circle planes and fault striae as arrows pointing toward the displacement of hanging wall rocks. These are lower hemisphere equal-area stereograms. Each plot also shows the calculated paleostress axes for each fault and striae couplet. The compression axes (P-axes) are red circles and the tension axes (T-axes) are blue-filled squares. The density of the T-axes are contoured by blue lines using Kamb contouring with a significance of 2 and a contour interval of 1% (calculated and plotted using FaultKinWin of R. Allmendinger). The yellow stars denote one or more maxima in T-axes orientations from the Kamb density contours. Fig. 7a. Faults and striae with low (rake < 30°) rakes. Fig. 7b. Faults and striae with medium (30° < rake < 60°) rakes. Fig. 7c. Faults and striae with high (rake > 60°) rakes. Fig. 7d. Faults with dominantly strike-slip (rake < 45°) rakes and striae with right-lateral slip. Fig. 7e. Faults with dominantly strike-slip (rake < 45°) rakes and striae with left-lateral slip. Fig. 7f. Paleostress axes calculated for all fault striae data. The stars denote the concentrations of T-axis orientations with the thick dark line denoting directions of the least compressive stress direction. The numbers next to the least compressive stress directions are the interpreted timing of stress orientations (see text of details).

plunging east-southeast and west-southwest (Fig. 7b). Strike-slip striae have a weakly defined maxima plunging shallowly west-southwestward and a strong maxima with a northwest trend and shallow plunge (Fig. 7a). The kinematic subsets of strike-slip component striae shows that the abundant right-lateral faults have a T-axes maximum trending northwest with shallow plunge (Fig. 7d) and the less common left-lateral striae have T-axes which plunge shallowly to the west-southwest (Fig. 7e).

INTERPRETATION

Paleostress

The T- and P-axes plots (Figs. 7a-e) show more than one maxima of T-axes orientations. Additionally, each slip and kinematic subset has distinctly different T-axes (Figs. 7e-a). Figure 7f has two main concentrations of T-axes: west-southwest/east-northeast and northwest/southeast. A third, less pronounced concentration is southwest/northeast.

Fault motion during one stress regime should have relatively consistent T and P-axes, even if there are active normal and strike slip faults. Multiple orientations of stress fields can be created by cyclic local stress fields due to loading and unloading by movement on local faults creating mutually cross-cutting relationships between faults and related fault sets. Alternatively, multiple stress fields may be due to changing stress directions by regional tectonic changes. Rearrangement of far-field stress fields could both create new faults in optimal orientations and reactivate older faults that have favorable orientations. The simplest explanation for the Rio Huizopa data is that several different stress regimes deformed this region since the Oligocene. Multiple, Oligocene and younger deformation events have been found or interpreted for the Sierra Madre Occidental and the surrounding region [see summaries in Gans (1997), Henry and Aranda-Gómez (2000), and Ferrari et al. (2007)]. The reactivation of earlier formed faults in a new and different stress fields is the simplest model to explain the numerous oblique-slip faults.

Relative timing of paleostress fields

Several observations in the Huizopa area support the hypothesis of distinctly different stress fields affecting this area. The northwest-striking, normal faults (Figs. 2 and 5) and north-striking right-lateral faults cut and offset the large, north-striking normal faults. The relationships between the two younger sets of faults in unclear. Another data set showing cross cutting relationships are the several fault exposures which preserve two fault striae directions. Many of these fault surfaces with two fault striae orientation are the large normal faults, which have earlier steeply plunging striae overprinted by younger more shallowly dipping striae (Figs. 8 and 9). The exposure in Figure 8 shows a crenulated, silicified fault surface which has steeply plunging fault striae which are parallel to the mullion fold axes. An oblique set of fault striae overprints the mullions and parallel fault striae only occur on one limb of the mullions. The overprinting fault striae data (Fig. 9a) is a small dataset, but the order of cross-cutting timing relationships is in agreement with mapped cross-cutting relationships: (1) the oldest striae are northerly and southerly striking normal faults with southeast- and northwest-trending fault striae, respectively; (2) then northerly and southerly striking normal faults with northeast- and southwest-trending fault striae, respectively; (3) then a north-northwest-striking fault with north-trending fault striae; and (4) lastly, northerly striking faults with north-trending fault striae with right-lateral kinematics. One steep northeast-striking fault has fault striae with a shallow rake overprinted by steep rake. This data divides the north/south striking normal faults into two separate fault striae categories.

To test the idea of these sequential deformations, the overprinting striae data are analyzed using their T- and P-axes (Fig. 9b). The different subsets of fault and fault striae couplets form relatively consistent orientations of T-axes: the earliest cross-cutting striae have west/east T-axes trends, followed by west-southwest/east-northeast, northeast (only one data point) and then northwest/southeast T-axes trends. This interpretation can be applied to the pattern of concentrations of T-axes in Figure 7f to derive the relative order of the least compressive stress orientations at Huizopa.

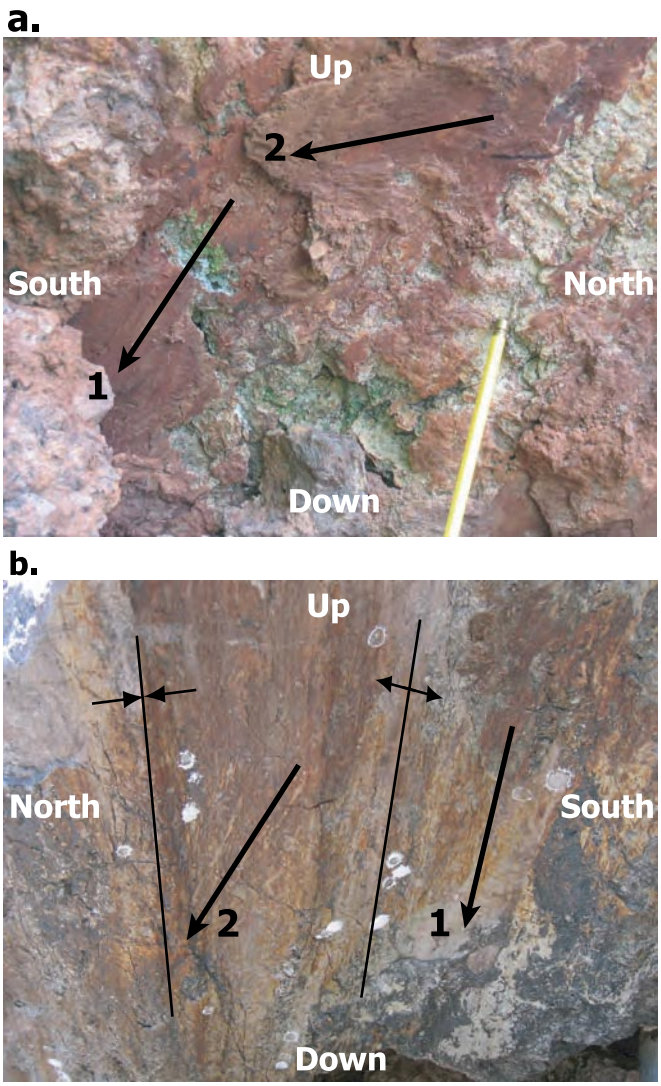

Figure 8. Detailed view of multiple overprinting fault striae on large normal fault slickenside surfaces near Rio Huizopa. The labeled thick black arrows indicate the two fault striae sets: 1 = earlier striae and 2 = overprinting striae. 8a. Looking down on a moderate, eastward dipping, northerly striking normal fault. The yellow pencil denotes the scale. Shallowly plunging right-lateral striae (denoted by '2') overprint steeply plunging normal offset striae (denoted by '1'). Note the gouge related to the second striae set fills in structural lows of mullions related to the first striae set. 8b. Upward view of underside of moderately plunging normal fault showing steeply-plunging striae (denoted by '1') overprinted by left-lateral oblique-normal offset striae (denoted by '2'). Note that the second striae set only occurs on the south limb of steeply-plunging slickensided synforms (traced out by arrows with a diverging arrows symbol) formed during earlier normal faulting (mullions). The view is approximately 1 m across.

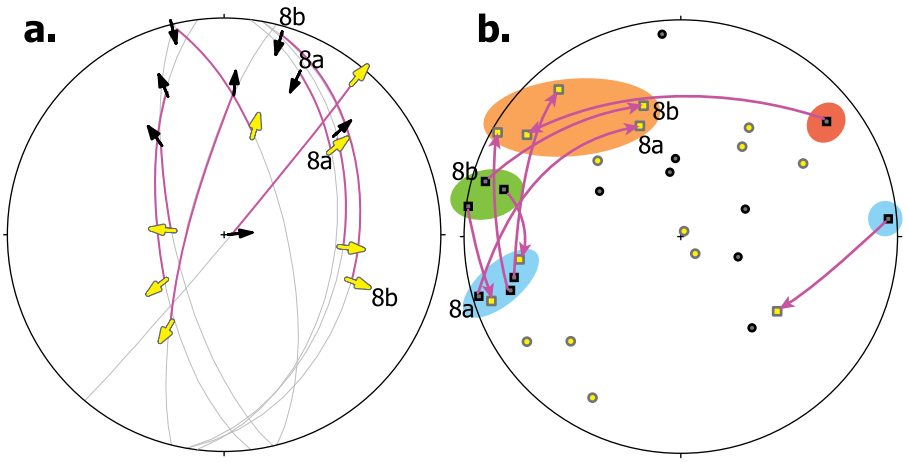

Figure 9. Overprinting fault striae data. 9a. Stereogram of great circle faults with two distinct sets of fault striae. Yellow short arrows are the first set of striae and the black short arrows are the second set of striae. Each set of striae on a fault (light gray great circle) has a purple line linking them together. 9b. Stereogram of calculated T- and P-axes, shown as squares and circles, respectively. The yellow stress axes are from the first set of striae and the black symbols are from the second set. Each set of T-axes is linked by a purple line pointing toward the second, younger T-axis. Distinct groups of orientations of T-axes are denoted by colored fields along with one uniquely oriented northeast-trending T-axis.

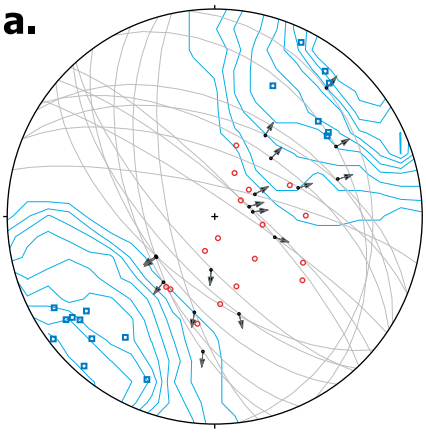

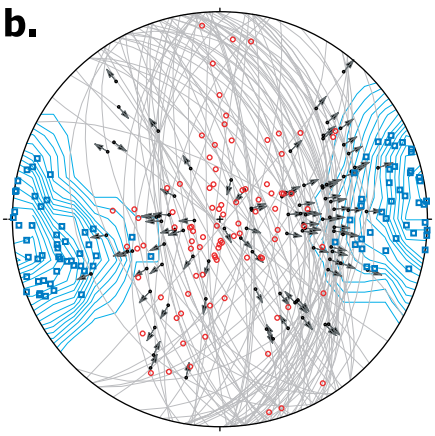

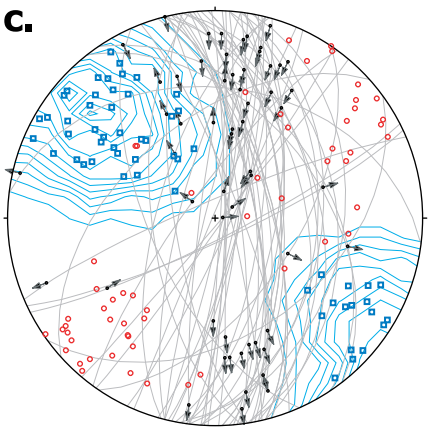

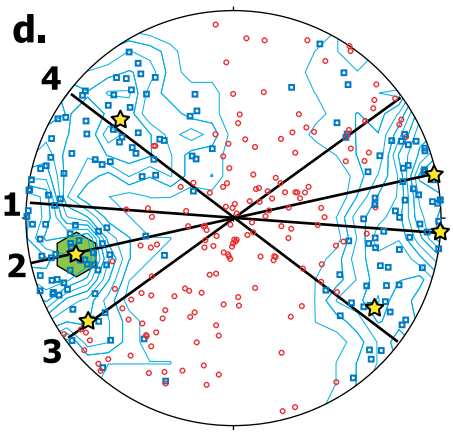

Figure 10. Kinematic subsets of fault striae and P- and T-axes data. See Figure 7 for symbol key. 10a. Great circle faults and fault striae with northeast- and southwest-trending T-axes. Fig. 10b. Great circle faults and fault striae with east- and west-trending T-axes Fig. 10c. Great circle faults and fault striae with southeast or northwest T-axes. Fig. 10 d. All of the fault-fault striae data. Distinct maxima of Kamb density contours are marked by yellow stars. The interpreted timing of these possible four deformation events is denoted by 1, 2, 3, and 4, with 1 being the earliest. The green hexagon shape marks the mean orientation for all of the poles to the dikes, veins and joints (Figs. 4b, c and d).

To further test the idea of the sequential deformation events interpreted from the overprinting striae and cross-cutting faults data the calculated stress data are be divided up into several subsets of T-axis orientation (Fig. 10). Distinct patterns of fault and fault striae orientations occur in these T-axes subgroups. The northeast/southwest T-axes (Fig. 10a) occur on dip and oblique slip faults which strike northwest/southeast dip steeply southwestward or steeply to gently northeastward. Many of the faults in this grouping are strongly oblique which may be explained by this deformation occurring after previous episodes of deformation which created structures which were reactivated in this later stress field. The west-northwest/east-southeast and west-southwest/east-northeast T-axes of Figure 9b are too close to separate and are considered together (Fig. 10b). These occur on dip slip and also oblique slip faults which strike north/south with steep westward dips or steep to gentle eastward dips. A few strike-slip faults oriented northwest/southeast and northeast/southwest occur with right-lateral and left-lateral kinematics, respectively. The northwest/southeast oriented T-axes (Fig. 10c) occur dominantly on north/south strike faults dipping steeply with right-lateral kinematics. There are a few west-southwest/east-northeast subvertical faults with left-lateral kinematics. Both sets of steeply dipping faults have mostly normal-oblique slip with lesser numbers of pure strike slip. One last set of faults in this T-axes subgroup are northeast/southwest striking faults with normal fault kinematics.

The west-southwest/east-northeast oriented T-axes (Fig. 10b) correspond directly to many geologic features at Huizopa. Most of the dikes (Fig. 4b) have similar tension orientations. These dikes are feeders to the upper volcanic strata here, thus this stress field was synchronous with at least the latest stage volcanism here. Veins and joints (Figs. 4c and d) have a similar west-southwest/east-northeast tensional axis as the dikes, but with more scatter to other orientations. Lastly, the bedding and flow foliations have strike and dips which could have resulted from ~25° tilting toward the west-southwest (Fig. 4a), assuming these volcanics to have been originally subhorizontal. The amount and tilt direction of the bedding and flow foliation correlate with the orientation and kinematics of the large normal faults which have. These moderately to gently eastward dipping normal faults were active during west-southwest/east-northeast tension (Fig. 10b) and have dips which are anomalously low (Jackson and White, 1989). The normal faults and volcanic strata are all tilted 20-30° to the west, with rotation about a horizontal axis. This domino-style normal fault system may have a master detachment or ductile flow at depth as in the rolling hinge, large–magnitude normal fault model of Wernicke and Axen (1988). The other two stress fields (Fig. 10a and c) are not associated with the dikes and appear to be younger that all of the pre-Quaternary geologic units at Huizopa.

The stress evolution at Rio Huizopa is interpreted using a simple Mohr-Coulomb model to have four distinct stress fields which have created four distinct sets of fault and fault striae couplets. (1) The earliest stress field is east-west least compressive stress creating several normal faults during deposition and volcanism of the lower and middle volcanic-volcaniclastic succession. (2) During at least the deposition and volcanism of the upper volcanic-volcaniclastic succession the least compressive stress direction shifted to a west-southwest/east-northeast direction during which numerous structures were formed or reactivated: the large normal faults, dikes, veins, and joints. The strata and the large normal faults were rotated ~25° to the west-southwest during this event. (3) northwest-trending normal faults formed during a deformation with least compressive stress directions orientated to the southwest/northeast. (4) the latest deformation of northerly right-lateral strike-slip faulting occurred during an event of northwest/southeast oriented least compressive stress.

CONCLUSIONS

The result of this study in the remote northern Sierra Madre Occidental is a relative chronology of multiple deformation events from inferred changing stress fields (Fig. 11). No deformation of Holocene sediments was noted and so the deformation here is presumed to have occurred between Oligocene and pre-Holocene.

Deformation events similar to these four deformations were noted in previous studies in nearby regions. West-southwest extension, including core complex formation, is noted from many areas farther west in Sonora from 20 to 16 Ma [see summaries in Gans (1997) and Ferrari et al. (2007)]. This episode is interpreted to coincide with the last stages of Oligocene arc volcanism. The Rio Huizopa area has a similarly oriented deformation that fits with this Oligocene-Miocene extension: the system of rotated normal faults which have displacements of a several hundreds of meters for a significant amount of west-southwest/east-northeast extension. A younger (from 12 to 6 Ma) event of approximately east-west extension also affected the Rio Yaqui area, 50 km to the southwest (McDowell et al., 1997; see also regional summary by Henry and Aranda-Gómez, 2000). This younger episode is not obvious at Rio Huizopa, but its presence can not be ruled out based on the current data. Many localities in the surrounding region are noted to have a younger set of north-northwest striking right-lateral faults. Gans (1997) mentions these structures as possibly accommodating many tens (or more) of kilometers of right-lateral displacement across Sonora. Many of the north- to north-northwest-striking faults on the geologic maps of the states of Sonora and Chihuahua (Servicio Geológico Mexicano, 2004a, 2004b) may be such right-lateral faults or older faults reactivated with strike-slip or oblique-slip kinematics. Age and kinematic data are sparse for these faults, but many are probably less than 5.5 Ma (Lonsdale, 1991). These right-lateral faults seem to accommodate a portion of the strain from the early Gulf extensional province.

This study at Rio Huizopa finds a similar Cenozoic tectonic evolution to nearby areas and does not preserve

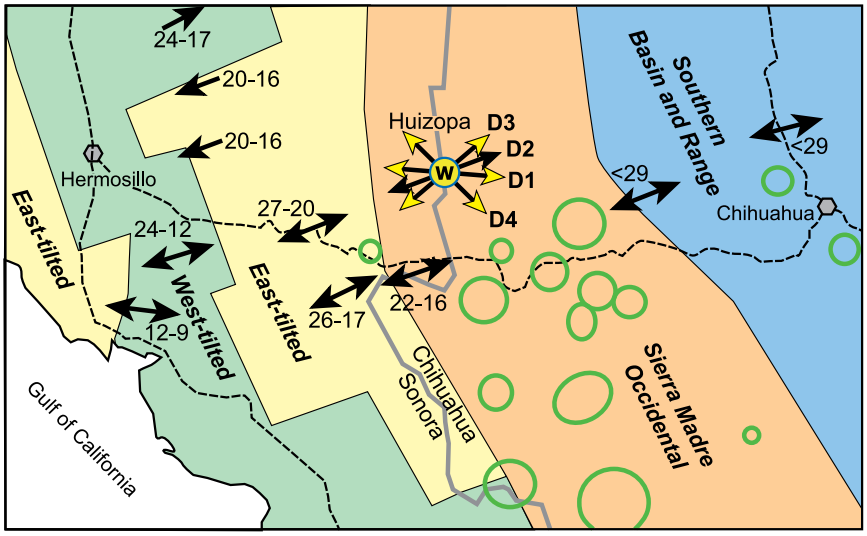

Figure 11. Map of orientations (black arrows, which indicate overall extension directions) and ages of major extension in the northern Sierra Madre Occidental [modified from Gans (1997) and Ferrari et al. (2007); see Ferrari et al. (2007) for references]. Geologic provinces are shown by the colored fields, with the Gulf Extensional province divided up into distinct tilt regimes. Large Oligocene calderas are shown as green circles. The interpreted temporal evolution of least compressive stress directions from Huizopa are plotted as four double-headed arrows (yellow and black-colored) labeled D1 to D4, with D1 being the oldest. The D2 stress direction (shown with a black double-headed arrow) is similar to the extension directions to most of the previously studied areas across this area, including the large magnitude extension in central Sonora. The westward tilt direction for the Huizopa is denoted by the 'W'.

unfaulted, ubiquitous, thick ignimbrites and numerous calderas that have previously characterized of the studies of the Cenozoic history of the Sierra Madre Occidental. Instead the Rio Huizopa area appears to link the deformation history of the regional events in the Sierra Madre Occidental, Southern Basin and Range and Gulf Extensional province. This area also provides a physical link between the deformations previously noted east and west of the Sierra Madre Occidental.

The definition of the Sierra Madre Occidental should be updated to include these new observations or the boundaries of the Sierra Madre Occidental need to be redefined to account for the abundant Cenozoic deformation found in the Rio Huizopa area.

ACKNOWLEDGMENTS

I thank J.L. Christman of Minera Sol de Oro, S.A. for permission to release this data. I also thank Manuel Mireles for assistance with field work.

REFERENCES CITED

Dickinson, W.R., 2006, Geotectonic evolution of the Great Basin: Geosphere, v. 2, n. 7, p. 353-368.

Ferrari, L., Valencia-Moreno, M. and Bryan, S., 2007, Magmatism and tectonics of the Sierra Madre Occidental and its relation with the evolution of the western margin of North America, *in* Alaniz-Álvarez, S.A. and Nieto-Samaniego, Á.F., eds., Geology of Mexico: Geological Society of America Special Paper 422, p. 1-39.

Fink, J. H. and Manley, C. R., 1987, Origin of pumiceous and glassy textures in rhyolite flows and domes: Geological Society of America Special Paper 212, p. 77-88.

Gans, P. B., 1997, Large-magnitude Oligo-Miocene extension in southern Sonora: Implications for the tectonic evolution of northwest Mexico: Tectonics, v. 16, p. 388-408.

Henry, C. D. and Aranda-Gómez, J. J., 1992, The real southern Basin and Range: Mid- to late Cenozoic extension in Mexico: Geology, v. 20, p. 701-704.

Henry, C. D. and Aranda-Gómez, J. J., 2000, Plate interactions control middle-late Miocene, proto-Gulf and Basin and Range extension in the southern Basin and Range: Tectonophysics, v. 318, p. 1-26.

Jackson, J.A. and White, N.J., 1989, Normal faulting in the upper continental crust: observations from regions of active extension: Journal of Structural Geology, v. 11, p. 15-36.

Lonsdale, P., 1991, Structural patterns of the Pacific floor offshore of peninsula California, *in* Dauphin, J.P, and Simoneit, B.R.T., eds., The Gulf and Peninsular Provinces of the Californias: American Association of Petroleum Geology Memoir 47, p. 87-125.

McDowell, F.W., and Keizer, R.P., 1977, Timing of mid-Tertiary volcanism in the Sierra Madre Occidental between Durango City and Mazatlan, Mexico: Geological Society of America Bulletin, v. 88, p. 1479-1486.

McDowell, F.W., Roldán-Quintana, J. and Amaya-Martínez, R., 1997, Interrelationship of sedimentary and volcanic deposits associated with Tertiary extension in Sonora Mexico: Geological Society of America Bulletin, v. 109, p. 1349-1360.

Servicio Geológico Mexicano, 2000, Carta geológico-minera Tecoripa, H12-12 Sonora-Chihuahua (1:250,000): Servicio Geológico Mexicano, scale 1:250,000, 1 sheet.

Servicio Geológico Mexicano, 2004a, Carta Geológico Estado de Chihuahua: Servicio Geológico Mexicano, scale 1:500,000, 1 sheet.

Servicio Geológico Mexicano, 2004b, Carta Geológico Estado de Sonora: Servicio Geológico Mexicano, scale 1:500,000, 1 sheet.

Stewart, J.H., 1978, Basin-range structure in western North America, a review, *in* Smith, R.B. and Eaton, G.P., eds., Cenozoic tectonics and regional geophysics of the western Cordillera: Geological Society of America Memoir 152, p. 1-13.

Stewart, J.H., 1998, Regional characteristics, tilt domains, and extensional history of the later Cenozoic Basin and Range Province, western North America, *in* Faulds, J.E. and Stewart, J.H., eds., Accommodation zones and transfer zones: the regional segmentation of the Basin and Range Province: Geological Society of America Special Paper 323, p. 47-74.

Wernicke, B. and Axen, G.A., 1988, On the role of isostasy in the evolution of normal fault systems: Geology, v. 16, p. 848–851.